Organic Electronics 13 (2012) 1023–1030

Contents lists available at SciVerse ScienceDirect

Organic Electronics

journal homepage: www.elsevier.com/locate/orgel

All-solution processed polymer light-emitting diodes with air stable metal-oxide electrodes

P. de Bruyn [a,b,*], D.J.D. Moet [a,c], P.W.M. Blom [a,c]

[a] Molecular Electronics, Zernike Institute for Advanced Materials, University of Groningen, Nijenborgh 4, 9747 AG Groningen, The Netherlands
[b] Dutch Polymer Institute, 5600 AX Eindhoven, The Netherlands
[c] Holst Centre, High Tech Campus 31, 5605 KN Eindhoven, The Netherlands

ARTICLE INFO

Article history:
Received 11 October 2011
Received in revised form 6 February 2012
Accepted 11 February 2012
Available online 16 March 2012

Keywords:
Organic
LED
Solution processing
Metal oxide
Air stable

ABSTRACT

We present an all-solution processed polymer light-emitting diode (PLED) using spincoated zinc oxide (ZnO) and vanadium pentoxide (V_2O_5) as electron and hole injecting contact, respectively. We compare the performance of these devices to the standard PLED design using PEDOT:PSS as anode and Ba/Al as cathode. We show that the all-solution processed PLEDs have an equal performance as compared to the standard design directly after fabrication. However, the ambient stability of the PLEDs with spincoated transition metal oxide electrodes is exceptionally good in comparison to the standard design.

1. Introduction

Polymer light emitting diodes hold the promise of large-area lighting at low cost [1]. However to achieve low costs all material layers in the device, including the injecting contacts, should be deposited from solution to fully benefit from a cheap production method such as roll-to-roll processing. In practice this excludes the use of low work function metal contacts, since they generally have to be evaporated in vacuum and are extremely sensitive to oxygen and moisture. The use of these metals is necessary to ensure efficient electron injection into the lowest unoccupied molecular orbital (LUMO) of the light emitting polymer due to its low electron affinity of typically 2–3 eV. This low electron affinity of light-emitting polymers intrinsically provides a great challenge for the air stability of the electron injecting contact [2]. Transition metal oxides such as zinc oxide (ZnO) and titanium oxide (TiO_x) have proven to be promising candidates for overcoming this problem. Specifically, systems with *evaporated* molybdenum trioxide (MoO_3) as hole injecting contact and ZnO or TiO_x as electron injecting contact have been studied extensively [3,4]. The enhanced hole injection properties of MoO_3 compared to poly(3,4-ethylenedioxythiophene):poly(4-styrenesulfonate) (PEDOT:PSS), especially when injecting into polymers with very deep HOMO levels, has been abundantly proven in literature [5–10]. Furthermore, thermally evaporated vanadium pentoxide (V_2O_5) has been shown to provide an ohmic injecting contact to luminescent polymers and polymer:fullerene solar cells as well [11–14]. However, a big challenge to overcome is the realization of metal oxide electrodes that are processed from solution, combining efficient charge injection with air stability. A solution-based process to produce amorphous V_2O_5 has already been developed in the last century [15–17] and has recently been revisited and introduced as anode in organic solar cells by Larsen-Olsen et al. [18].

Here we introduce organic light emitting diodes with ZnO and V_2O_5 injecting contacts through a fully solution

* Corresponding author at: Molecular Electronics, Zernike Institute for Advanced Materials, University of Groningen, Nijenborgh 4, 9747 AG Groningen, The Netherlands. Tel.: +31 50 363 5211.
E-mail address: p.de.bruyn@rug.nl (P. de Bruyn).

1566-1199/$ - see front matter © 2012 Elsevier B.V. All rights reserved.
http://dx.doi.org/10.1016/j.orgel.2012.02.014

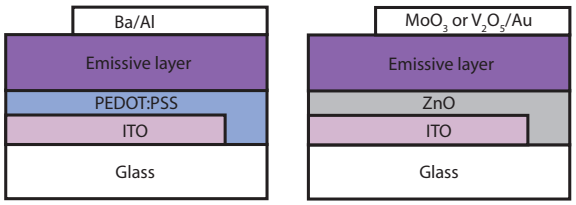

Fig. 1. Device structures of the devices presented in this study. Conventional structure (left) and inverted structure (right).

deposited and low temperature route. ZnO can be created through the spin casting and subsequent decomposition of zinc acetylacetonate ($Zn(acac)_2$) under ambient conditions and at low temperatures (130 °C) [19,20]. V_2O_5 is deposited by diluting vanadium oxytriisopropoxide in isopropanol and spin casting this solution in ambient conditions to yield a layer of V_2O_5. The procedure to create the V_2O_5 layer does not require post-processing heat treatment, making the entire process compatible with cheap flexible substrates such as PET. For the emitting polymer, we chose the polyfluorene copolymer poly[9,9-didecanefluorene-alt-(bis-thienylene)benzothiadiazole] (PF10TBT). An advantage of this red-emitting polymer compared to for example a poly(*p*-phenylene vinylene) (PPV) based polymer is its higher electron affinity. Its LUMO is located typically 3.4 eV below vacuum (as compared to 2.9 eV for PPV), making it easier to inject electrons from the ZnO cathode, which has a work function of typically ~4 eV. Furthermore, PF10TBT exhibits a good ambient stability allowing us to demonstrate the stability of the contacts and to distinguish between contact and polymer degradation upon exposure to air. In Fig. 1 the device layouts of the various devices presented in this study are shown. From here on the architecture with an evaporated low work function electron injecting metal top contact will be denoted by 'conventional' and the PLEDs with the metal oxide contacting scheme will be denoted by 'inverted'. We show that the performance of the inverted style devices with solution processed ZnO and V_2O_5 contacts is equivalent to the performance of the conventional devices, while device stability during storage and operation in air is greatly enhanced. This approach therefore paves the way towards all-solution processed and stable polymer LEDs.

2. Experimental

All devices were prepared on ITO patterned glass substrates. Substrates were cleaned with non-ionogenic detergent before being rinsed in a de-ionized water flowbath. Next the substrates were sonicated in acetone and isopropanol, followed by dry spinning and drying in an oven at 140 °C for 10 min. Finally the substrates were subjected to UV–ozone cleaning for 20 min. PEDOT:PSS was spin cast from a water based suspension (Clevios P VP AI 4083) under ambient conditions and dried in an oven at 140 °C for 10 min. ZnO was deposited from a precursor solution of zinc acetylacetonate of 20 mg/ml in ethanol ($Zn(acac)_2$), followed by conversion to ZnO at 130 °C, yielding layer thicknesses of 15–20 nm. PF10TBT was spin cast from a chloroform solution of 12 mg/ml at various rates to obtain films between 50 and 100 nm. V_2O_5 layers were made by diluting vanadium oxytriisopropoxide 1:50 by volume in isopropanol and spin casting to yield layers of 15 nm of V_2O_5. All solution processing and annealing steps are done under ambient conditions. MoO_3, Au, Ba and Al were thermally evaporated in a vacuum chamber at pressures of $<10^{-6}$ mBar. *I–V* measurements were done with a computer controlled Keithley 2400 Sourcemeter. Devices are made with 4 sizes ranging from 10 mm^2 to 1 cm^2 on one substrate. For the stability measurements stored devices refer to devices on the same substrate not operated in air.

3. Results and discussion

3.1. Evaluation of the spincoated ZnO cathode

In order to evaluate the performance of the spincoated ZnO cathode and V_2O_5 anode separately we first make use of a test device (Fig. 1). This inverted device contains a spincoated ZnO cathode as bottom contact and an evaporated MoO_3/Au hole injecting contact as top contact. This evaporated MoO_3/Au anode has been proven to be an Ohmic contact on polyfluorene derivatives with a very deep HOMO level (−6.0 eV below vacuum). [5] As a result also on the PF10TBT polymer studied here, with the HOMO level at −5.4 eV, we can be sure that this hole contact is ohmic, enabling to investigate the performance of the spincoated ZnO cathode. As a first step the electrical characteristics of the inverted devices with a solution processed ZnO electron injecting bottom contact and an evaporated MoO_3/Au hole injecting top contact are compared to conventional devices with a PEDOT:PSS and Ba/Al contact for hole and electron injection, respectively. Fig. 2 shows the current density–voltage (*J–V*) and light-output–voltage (*L–V*) characteristics (Fig. 2a), as well as the ratio of the light output and the current as a function of voltage (Fig. 2b), which is a measure for the PLED efficiency. The inset of Fig. 2b shows the current of the devices on a double log scale.

First of all, what can be discerned is close congruence between the efficiencies of the two architectures. This is a strong indication that the electron injection is efficient and that the ZnO forms an ohmic electron contact on PF10TBT. This is further confirmed by the fact that after correction for the built-in voltage the current densities of the conventional and inverted devices are equal and, as shown in the inset of Fig. 2b, follow a space-charge limited trend, suggesting ohmic injecting contacts in both cases.

For a PLED with ohmic contacts the current density in the plasma limit is given by [21]:

$$J = \left(\frac{9\pi}{8}\right)^{1/2} \varepsilon_0 \varepsilon \left(\frac{2q\mu_p\mu_n(\mu_p+\mu_n)}{\varepsilon_0\varepsilon B}\right) \frac{(V-V_{bi})^2}{L^3} = \frac{9}{8}\varepsilon_0\varepsilon\mu_{eff}\frac{(V-V_{bi})^2}{L^3}, \quad (1)$$

with *J* the current density, ε_0 the permittivity of vacuum, ε the relative dielectric constant of the polymer, μ_p and μ_n the hole and electron mobility, *B* the bimolecular recombi-

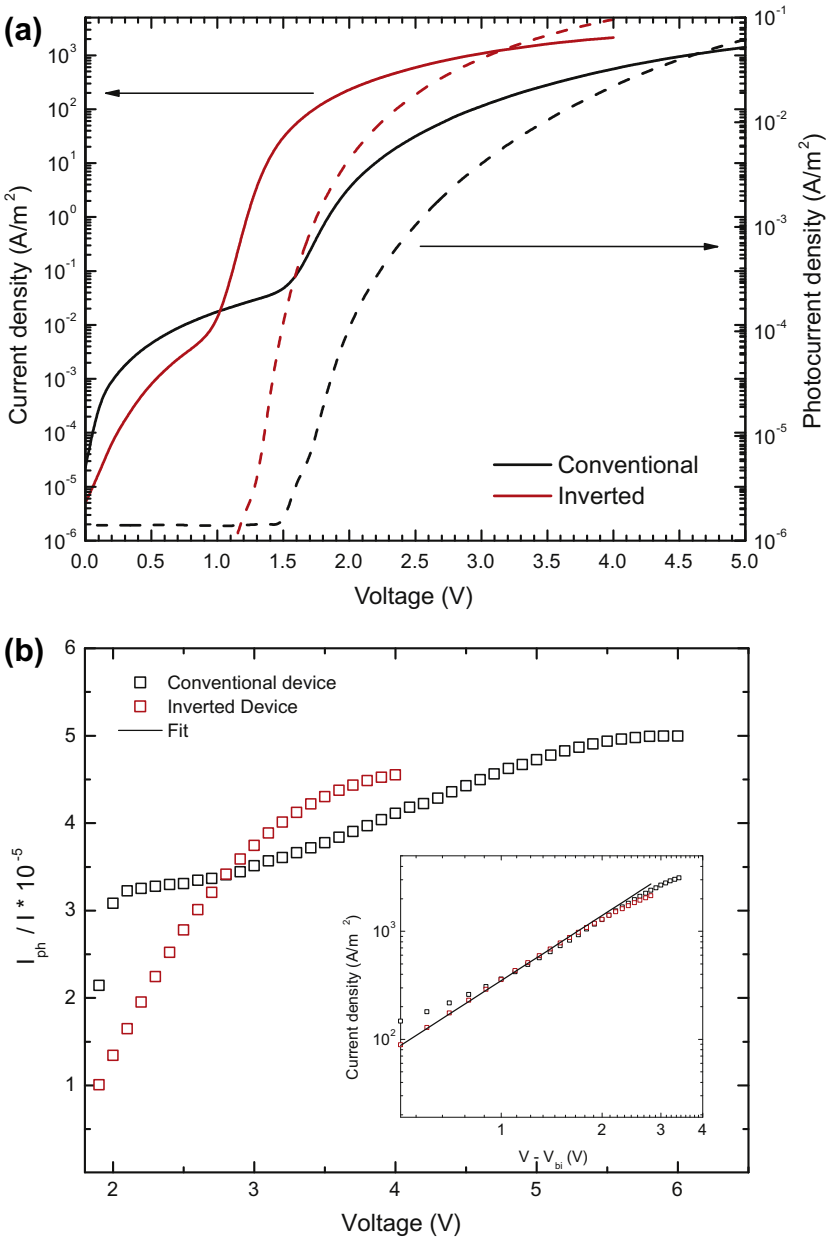

Fig. 2. Performance comparison of the conventional and inverted LEDs. (a) Comparison of *J–V* (solid lines) and *L–V* (dashed lines) characteristics and (b) relative PLED efficiency. The inset of (b) shows the current on a log–log scale, as well as a fit to the space charge limited current model of Eq. (1).

nation constant, V the applied voltage and L the thickness of the polymer layer. Taking $\varepsilon = 3$ and $L = 80$ nm, the effective mobility μ_{eff} derived in this fashion amounts to 6.0×10^{-9} m^2/Vs, in agreement with previous determinations [22]. Furthermore, a decrease in the turn-on voltage is observed, as previous publications have shown as well [3]. The exact origin of the decrease in the turn-on voltage is still under investigation. In the standard metal–insulator-metal model it would imply a decrease in the difference between the work functions the contacts in these devices. In that case small contact barriers would be present in the device. The current–voltage and efficiency–voltage characteristics, however, show an efficient charge injection for this specific combination of light-emitting polymer and contacts. In a recent study (M. Lu et al. submitted to JAP) we found that holes injected from the anode get trapped at the ZnO/semiconductor interface. The resulting electric field enhances the injection of electrons from the ZnO in the polymer, explaining the good efficiencies. Next we consider the ambient stability of these devices under two conditions, (a) storage in air and (b) operation in air. Fig. 3a and b shows the pristine and the *J–V* characteristics after 24 h of storage in air of the conventional and inverted devices, respectively. The normal geometry device has lost most of its functionality after 24 h of storage in air, while the inverted geometry device remains intact. Besides the

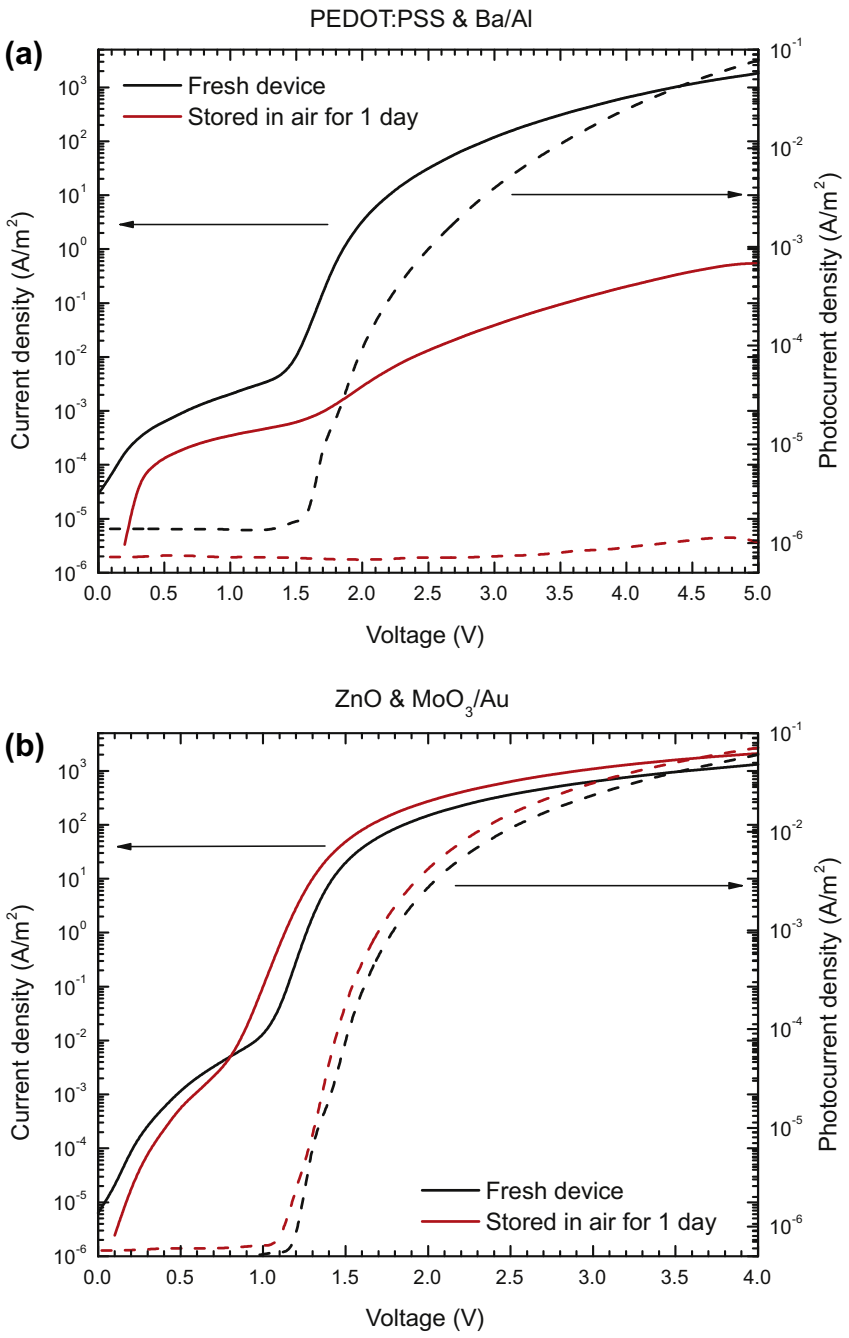

Fig. 3. Storage stability of (a) conventional and (b) inverted geometry devices. Shown are the *J–V* and *L–V* curves in both cases.

storage stability, also the operational stability is essential. Fig. 4a and b shows the *J–V* curves for pristine devices and after operation in air for 24 h at 10^3 A/m^2 for conventional and inverted geometry LEDs, respectively. The conventional device degrades rapidly in air as a consequence of the deteriorating properties of the electron injecting Ba contact upon exposure to air. After 24 h the conventional device has ceased functioning. This degradation is related to rapid degradation of the barium contact layer. After deposition a $BaAl_4$ alloy is formed at the interface with the polymer [23]. Upon exposure to water that penetrates through the pinholes in the Al cover layer an insulating $Al(OH)_3$ layer is formed at the interface. This layer effectively prevents electron injection and therefore kills the electroluminescence, leading to the formation of black spots. The inverted device however maintains a high current density and light output. Since the emitting polymer layer is identical in both cases, the only conclusion is that

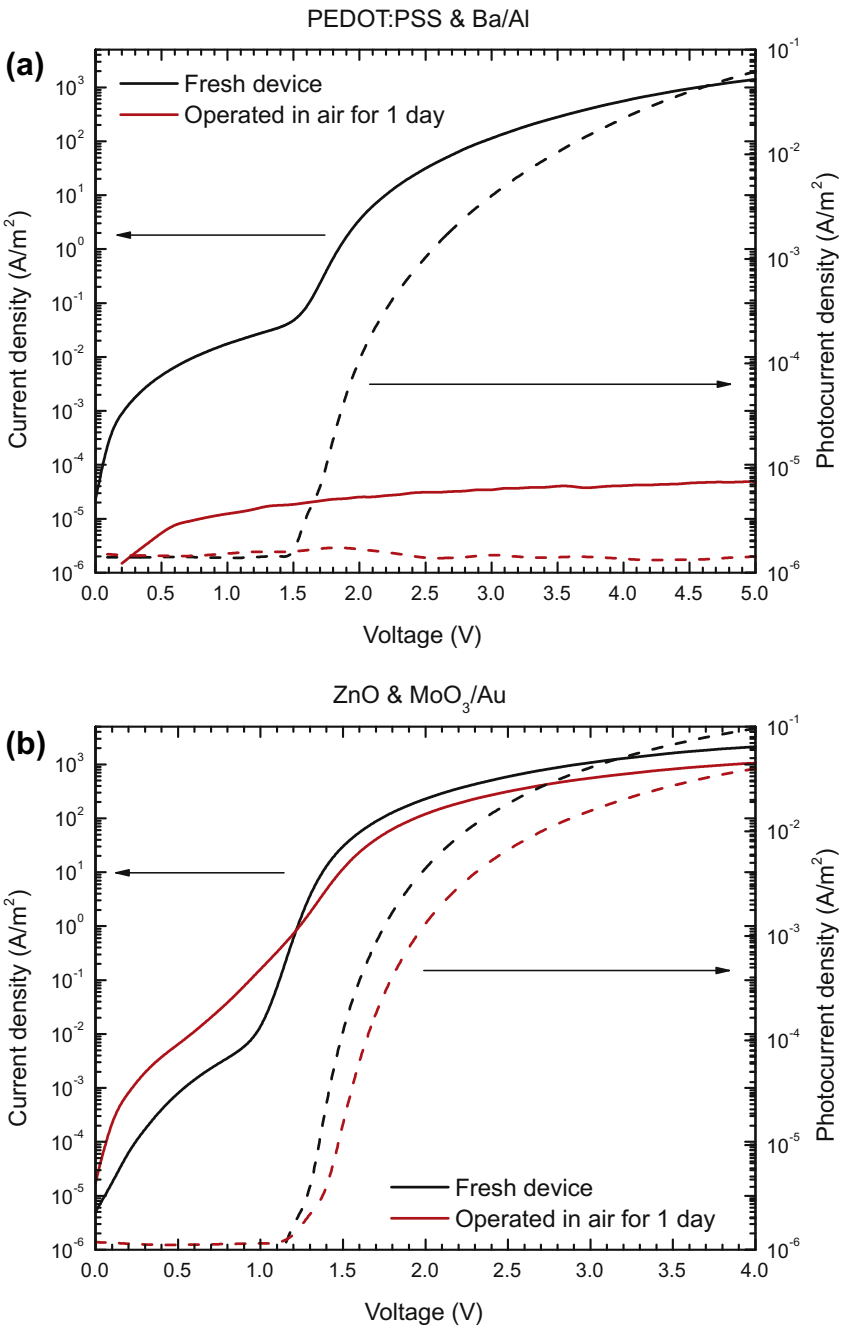

Fig. 4. Operational stability of (a) conventional and (b) inverted geometry devices. Shown are the *J–V* and *L–V* curves in both cases.

the differences in degradation behavior are caused by the difference in contacts. Therefore the metal oxide contacts show excellent ambient stability in injecting charges, compared to the conventional contacts. Besides this quantitative difference, Fig. 5 also shows the deterioration qualitatively. Depicted are photographs of the devices operating in ambient conditions after set periods of time. Both devices were consistently captured in a single frame for equal lighting conditions, as well as being operated at the same initial current density of 10^3 A/m^2. The formation of dark areas of zero electroluminescence can clearly be seen in the conventional device, starting mere minutes after exposure to air, eventually breaking down completely after approximately 19 h. The distinctive nucleation of these spots and their growth can evidently be seen on the photographs. In contrast, the inverted geometry device remains uniform, in agreement with the results obtained from the electrical measurements. We can therefore conclude that the spin-

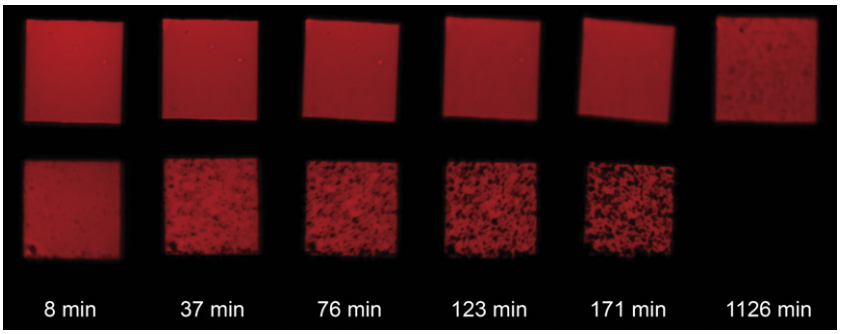

Fig. 5. Digital photographs of operated devices under ambient conditions. The top row shows the inverted devices, while the bottom row shows the conventional devices.

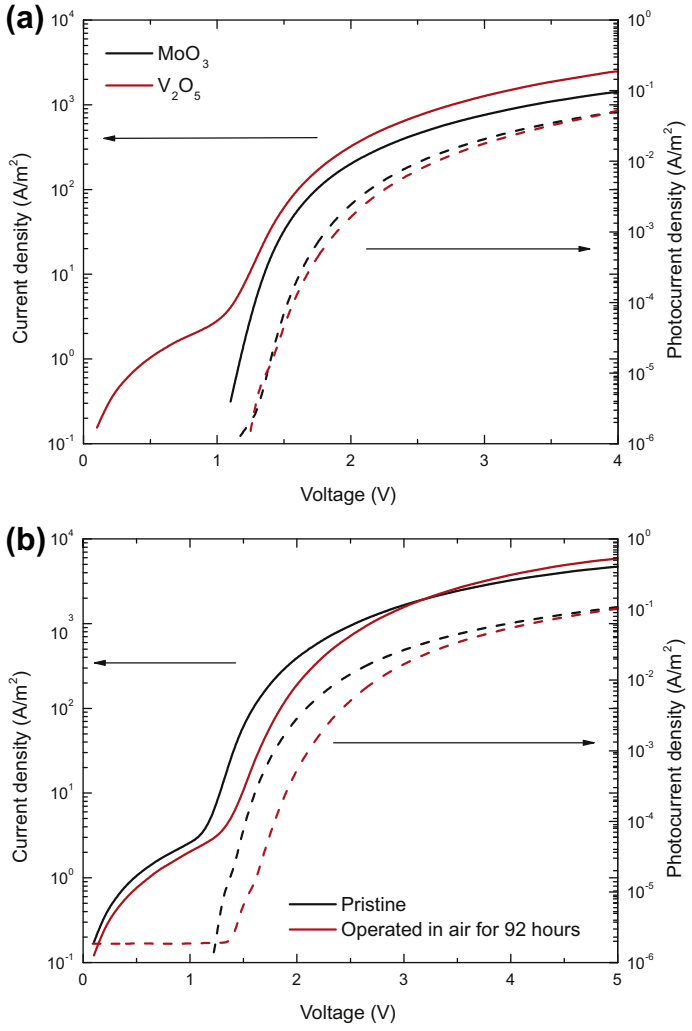

Fig. 6. Performance comparison of the devices with anodes based on MoO_3 and V_2O_5. (a) *J–V* and *L–V* characteristics. (b) Operational stability of V_2O_5 devices, shown are curves before and after 92 h of operation in air.

coated ZnO bottom cathode injects electrons efficiently into PF10TBT and also exhibits excellent air stability as compared to the commonly used thermally evaporated low work function metal electrodes.

3.2. Evaluation of the solution processed V_2O_5 anode

Finally we compare the characteristics of the fully solution processed system with a spincoated V_2O_5 anode to the

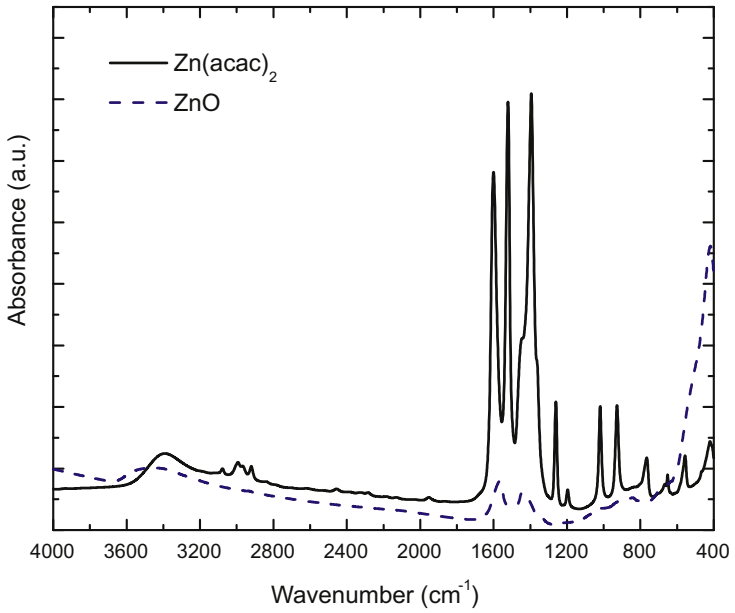

Fig. 7. FTIR measurements on $Zn(acac)_2$ and ZnO layers, showing the emergence of the Zn–O bond feature at 418 cm^{-1} after annealing, as well as the presence of presumably a surface hydrozincite species.

reference device with the evaporated MoO_3 anode. Fig. 6a shows a comparison of the *J–V* characteristics of the two devices, as well as the *J–V* curves of the V_2O_5 based LED in its pristine state and after operation in air for approximately 92 h in Fig. 6b. The performance of the two systems is remarkably similar. The current density is even slightly higher for the solution processed V_2O_5 device, due to a slightly thinner polymer layer. The electrical characterization clearly shows that both materials give an ohmic hole injecting contact to the polymer highest occupied molecular orbital (HOMO). Similar stability to the evaporated MoO_3 LED can be observed in the V_2O_5 devices, showing only little degradation after 92 h of operation in ambient conditions, further exemplifying the excellent air stability of metal oxide materials. As a result an all-solution processed PLED with two ohmic contacts has been realized. The fact that these PLEDs are also stable in air for various hours without encapsulation is beneficial for a roll-to roll production process. It implies that the PLEDs can first be processed roll-to-roll from solution and that later on a barrier foil can be laminated to the device. Another intriguing question is what kind of requirements with regard to the water vapor transmission rate of the barrier stack are needed for this type of all-solution processed PLEDs, which is a subject of further research.

3.3. Characterization of the spincoated ZnO cathode

To address the chemical properties of the spin cast ZnO layer, Fourier transform infrared spectroscopy (FTIR) measurements were performed on these films. Fig. 7 shows the mid-infrared spectrum of a film of the $Zn(acac)_2$ precursor and a typical ZnO film. Several features can be distinguished. The vibrations of $Zn(acac)_2$ around 3000–3400 cm^{-1} and in the range 400–1600 cm^{-1} are well documented and correlate to the peak positions found here [24]. After conversion to ZnO we see a clear peak appearing at 418 cm^{-1}, that originates from the Zn–O vibration peak, demonstrating that indeed ZnO has formed. Furthermore, additional features in the ZnO spectrum appear between 800 and 1600 cm^{-1}. These features can be identified as a hydrozincite species, which can easily form on ZnO under ambient conditions, as described in literature [25]. From the good performance of both solar cells (Ref. [19]) and PLEDs presented here with this precursor ZnO we can conclude that the hydrozincite species does not hinder the electrical properties.

4. Conclusions

An all-solution processed PLED has been realized with spin coated metal oxide contacts. The performance of these PLEDs is equivalent to the performance of conventional PLEDs with a PEDOT:PSS anode and a thermally evaporated low work function metal electron injecting contact. The ambient stability of the all-solution processed PLEDs is greatly enhanced as compared to the devices with the conventional architecture. The results presented here promise a low cost, universal and facile solution based production process for PLEDs using air stable metal oxide contacts.

Acknowledgements

The authors would like to acknowledge the Dutch Polymer Institute for funding through DPI Project #660. Furthermore the authors are grateful for technical support of J. Harkema and F. van der Horst.

References

[1] S. Reineke, F. Lindner, G. Schwartz, N. Seidler, K. Walzer, B. Lussem, K. Leo, Nature 459 (2009) 234–238.
[2] D.M. de Leeuw, M.M.J. Simenon, A.R. Brown, R.E.F. Einerhand, Synth. Met. 87 (1997) 53–59.
[3] H.J. Bolink, E. Coronado, D. Repetto, M. Sessolo, Appl. Phys. Lett. 91 (2007) 223501–223503.
[4] K. Morii, M. Ishida, T. Takashima, T. Shimoda, Q. Wang, M.K. Nazeeruddin, M. Graetzel, Appl. Phys. Lett. 89 (2006) 183510–183513.
[5] H.T. Nicolai, G.A.H. Wetzelaer, M. Kuik, A.J. Kronemeijer, B. de Boer, P.W.M. Blom, Appl. Phys. Lett. 96 (2010) 172107–172113.
[6] H. You, Y. Dai, Z. Zhang, D. Ma, J. Appl. Phys. 101 (2007) 026105–026113.
[7] T. Matsushima, Y. Kinoshita, H. Murata, Appl. Phys. Lett. 91 (2007) 253504–253513.
[8] T. Matsushima, H. Murata, J. Appl. Phys. 104 (2008) 034507–034514.
[9] H.J. Bolink, E. Coronado, D. Repetto, M. Sessolo, E.M. Barea, J. Bisquert, G. Garcia-Belmonte, J. Prochazka, L. Kavan, Adv. Funct. Mater. 18 (2008) 145–150.
[10] M. Kroger, S. Hamwi, J. Meyer, T. Riedl, W. Kowalsky, A. Kahn, Appl. Phys. Lett. 95 (2009) 123301–123303.
[11] G. Li, C.-W. Chu, V. Shrotriya, J. Huang, Y. Yang, Appl. Phys. Lett. 88 (2006) 253503–253513.
[12] V. Shrotriya, G. Li, Y. Yao, C.-W. Chu, Y. Yang, Appl. Phys. Lett. 88 (2006) 073508–073513.
[13] S. Tokito, K. Noda, Y. Taga, J. Phys. D: Appl. Phys. 29 (1996) 2750.
[14] K. Takanezawa, K. Tajima, K. Hashimoto, Appl. Phys. Lett. 93 (2008) 063308–063313.
[15] W. Prandtl, L. Hess, Z. Anorg. Chem. 82 (1913) 103–129.
[16] J. Livage, Chem. Mater. 3 (1991) 578–593.
[17] J. Livage, Solid State Ionics 86–88 (1996) 935–942.
[18] T.T. Larsen-Olsen, E. Bundgaard, K.O. Sylvester-Hvid, F.C. Krebs, Org. Electron. 12 (2011) 364–371.
[19] P. de Bruyn, D.J.D. Moet, P.W.M. Blom, Org. Electron. 11 (2010) 1419–1422.
[20] T. Arii, A. Kishi, J. Therm. Anal. Calorim. 83 (2006) 253–260.
[21] M.A. Lampert, P. Mark, Current Injection in Solids, Academic, New York, 1970.
[22] D.J.D. Moet, M. Lenes, J.D. Kotlarski, S.C. Veenstra, J. Sweelssen, M.M. Koetse, B. de Boer, P.W.M. Blom, Org. Electron. 10 (2009) 1275–1281.
[23] C.W.T. Bulle-Lieuwma, P. van de Weijer, Appl. Surf. Sci. 252 (2006) 6597–6600.
[24] A.M.A. Bennett, G.A. Foulds, D.A. Thornton, Polyhedron 8 (1989) 2305–2311.
[25] G.J. Millar, I.H. Holm, P.J.R. Uwins, J. Drennan, J. Chem. Soc., Faraday Trans. 94 (1998) 593–600.